Inorganic Chemistry, Vol. 17, No. 2, 1978 **297**

Contribution from the Department of Chemistry,
Tulane University, New Orleans, Louisiana 70118

Solution Structure and Reactivity of Hydridoiron Tetracarbonyl Anion, $[HFe(CO)_4]^-$

M. Y. DARENSBOURG,* D. J. DARENSBOURG,* and H. L. C. BARROS

Received May 22, 1977

A detailed analysis of intensities of CO stretching vibrational modes in bis(triphenylphosphine)iminium hydridotetracarbonylferrate suggests the $HFe(CO)_4^-$ to exist in tetrahydrofuran solution in the precise form as in the solid state, i.e., as a pseudo trigonal bipyramid with H in an axial position. Considerable deviation of $(OC)_{ax}$–Fe–$(CO)_{eq}$ angularity from 90° is observed both in the solid-state structure (99.1°) and in these solution studies (100°). Carbon-13 labeled CO incorporation into $PPN^+HFe(CO)_4^-$ was catalyzed by Na^+ ion-paired interaction and used to obtain precise frequency data for an accompanying force field calculation.

Introduction

The role of transition metal carbonyl anions continues to expand in organometallic chemistry. Concurrent with important studies in the use of metal carbonyl anions in organometallic synthesis by King,[1] in organic synthesis by Collman,[2] in the production of "superreduced" species by Ellis,[3] and in the development of methanolysis catalysts by Pettit[4] have been essential crystal structure determinations of Bau and his co-workers.[5] Furthermore, it appears that hydridometal carbonylates will continue to be a popular field of investigation, since their role in cluster catalysis is just beginning to be elucidated.[6]

We have been involved in a research program centered around probing the solution structure of organometallic salts by the tools of infrared spectroscopy and conductivity measurements.[7-10] This communication presents data on the salts of hydridotetracarbonylferrate.

Experimental Section

Preparations. The hydridoiron tetracarbonyl species was prepared from $Fe(CO)_5$ (0.5 mL, ~3.7 mmol) in methanol (2.5 mL) and NaOH (0.7 g, 17.5 mmol in 2.0 mL of H_2O) in Schlenkware under a nitrogen atmosphere. The reaction mixture was stirred for 30 min followed by addition of bis(triphenylphosphine)iminium chloride (2.1 g, 3.7 mmol in 5 mL of MeOH) with a yellow precipitate being formed immediately. Additional methanol (12.5 mL) was added and the reaction mixture was filtered. The $[PPN][HFe(CO)_4]$ was purified by recrystallization from EtOH/EtOAc to yield light golden crystals which were dried under vacuum.

Infrared Measurements. The infrared spectra of the $[PPN][HFe(CO)_4]$ complex were recorded on a Perkin-Elmer 521 spectrophotometer equipped with a linear absorbance potentiometer. The absorbance spectrum was recorded at a rate of approximately 15 cm^{-1} min^{-1} on an expanded scale. The spectra were calibrated against a water vapor spectrum below 2000 cm^{-1} and against a CO spectrum above 2000 cm^{-1}. Matched 0.1-mm sodium chloride cells were used in the measurements. Care was taken to ensure that all spectra were recorded using the same instrumental settings. Tetrahydrofuran solvent was distilled under N_2 from a purple 0.1 M sodium/benzophenone solution immediately prior to use.

For determining the intensities of the ν(CO) vibrations, the samples were prepared in the following manner. The samples were weighed on a Cahn electrobalance to ±0.01 mg and dissolved in an appropriate quantity of THF. Solution concentrations were in the range 9.57×10^{-4} to 5.40×10^{-2} M. Care was taken to exclude air from the solution, i.e., flamed volumetric flasks were serum-capped and flushed with nitrogen before addition of solvent. Similarly, samples were prepared as above with a calculated excess of $NaBPh_4$ being added prior to dissolution. The complexes were observed to be stable in solution during the course of the spectral measurements.

The intensities of the ν(CO) absorptions were determined using eq 1, where the intensity is expressed in units of M^{-1} cm^{-2}, c is the concentration in moles per liter, l is the cell path length in centimeters, and I_0 and I are the incident and transmitted apparent intensities. The areas of the band envelopes were determined with a planimeter and were reproducible to at least 1%. The concentration was plotted against (area)$2.303/l$ and the resulting straight line was optimized by the linear least-squares method (Figure 1). The slope of the line is the intensity of the stretching vibration.

$$\text{absolute intensity} = \frac{2.303}{cl}\int_{\text{band}} \log\frac{I_0}{I}\,d\nu = \frac{2.303}{cl} \times (\text{area of band envelope}) \quad (1)$$

Conductivity Measurements. Resistivities of tetrahydrofuran solutions of $PPN^+HFe(CO)_4^-$ of known concentration (range of 10^{-4}–10^{-6} M) were measured on a Barnstead conductivity bridge, Model PM 70CB, at 22 ± 0.3 °C. An exact quantity of THF was syringed into the empty conductivity cell chamber (cell constant = 0.238 cm^{-1}), and successive aliquots of the carbonylate solution were added via microliter syringe utilizing all precautions regarding air, moisture, and glassware contamination noted in our earlier works[8,9] in addition to excluding light. Nevertheless, results were less reproducible, and considerable drift in readings was encountered. The best data were analyzed according to the treatment for Fuoss Type IV electrolytes and according to the procedures outlined in earlier papers.[8,9] A range of ion-pair dissociation constants of 4.5×10^{-4} to 1.5×10^{-4} M was obtained from which a best estimate was taken as $\sim 2 \times 10^{-4}$ M.

Results and Discussion

Smith and Bau have reported the x-ray crystal structure parameters for $[HFe(CO)_4]^-$ as its bis(triphenylphosphine)iminium salt.[5a] The configuration of the anion is that of a distorted trigonal bipyramid with the hydride ligand occupying an axial position. Alternatively, the $Fe(CO)_4$ fragment of the anion may be described as intermediate between tetrahedral and trigonal bipyramidal. The iron atom is displaced 0.27 Å from the plane of the three equatorial carbonyl ligands.

Such a symmetry of the $[HFe(CO)_4]^-$ anion should lead to a fairly simple ν(CO) infrared pattern. The C_{3v} symmetry of the $Fe(CO)_4$ moiety predicts the three-band spectrum that is indeed observed for $[PPN][HFe(CO)_4]$ in tetrahydrofuran and the bands are assigned, in decreasing frequency, to the $A_1^{(2)}$, $A_1^{(1)}$, and E vibrational modes (Figure 2). It is immediately noted that the high-frequency A_1 vibration (composed to a large extent of equatorial carbonyl motion) is of very low intensity when compared to phosphine-substituted iron tetracarbonyl derivatives.[11] We have, therefore, undertaken a quantitative investigation of the infrared intensities of the CO stretching vibrations of $[HFe(CO)_4]^-$ in THF solution.

Carbonyl Stretching Force Constants in $[HFe(CO)_4]^-$. Force constants for the CO stretching vibrations in the $[HFe(CO)_4]^-$ anion were calculated initially employing a modified Cotton–Kraihanzel approach using the three observed frequencies ($A_1^{(2)}$, $A_1^{(1)}$, and E). The force constants k_1, k_2, k_c, and $k_{c'}$ (which refer to the axial, equatorial, equatorial–equatorial, and axial–equatorial constants, respectively) were calculated from the three frequencies assuming a ratio of $k_{c'}/k_c$ of 1.40. We have previously found this ratio for the interaction constants in a large number of phosphine-substituted L-$Fe(CO)_4$ complexes.[11] Nevertheless, as noted in Figure 2, in addition to the three principal ν(CO) absorptions ascribable

0020-1669/78/1317-0297$01.00/0

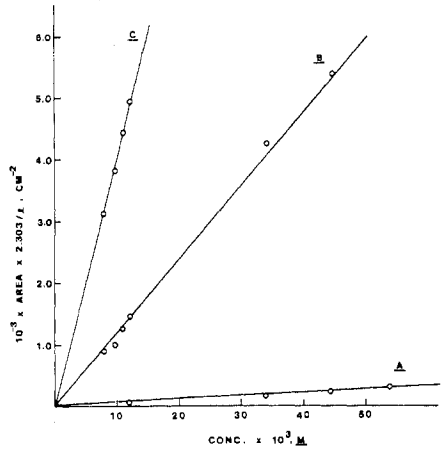

Figure 1. Plot of area × 2.303/l vs. concentration for A, $A_1^{(2)}$ band, B, $A_1^{(1)}$ band, and C, E band.

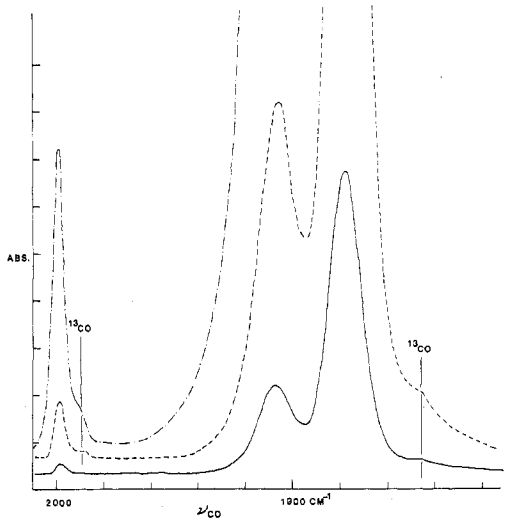

Figure 2. ν(CO) spectra of [PPN][HFe(CO)$_4$] in tetrahydrofuran solution. The bands due to natural abundance ^{13}CO are noted on the high-concentration spectra.

to the 2 A_1 + E vibrational modes of the $[HFe(CO)_4]^-$ species, there are two very weak ν(CO) bands observable at high concentrations due to natural abundance ^{13}CO. That is, these vibrations are attributed to the 3% of all hydridotetracarbonylferrate molecules which contain one equatorial ^{13}CO group. Confirmation of these ^{13}CO frequencies was obtained by enrichment of [PPN][HFe(CO)$_4$] with gaseous ^{13}CO. This process will be discussed later on in the paper. It is therefore possible to calculate the four CO stretching force constants employing the five measured frequencies making no assumption regarding the relative magnitudes of k_c and $k_{c'}$. Table I contains the observed and calculated ^{12}CO and ^{13}CO stretching vibrations for the $[HFe(CO)_4]^-$ species along with the computed CO stretching force field. These computations were performed with an interative program based on the work of Schachtschneider and Snyder.[12]

Absolute Infrared Intensities. The measured absolute infrared intensities of the three ν(CO) vibrational modes in $[HFe(CO)_4]^-$ are reported in Table II along with analogous phosphine and phosphite derivatives for comparison. The equations (2–4) listed below, which we have previously developed for $LFe(CO)_4$ species,[11,13] relate the measured band intensities to the group MCO dipole moment derivatives. G_{tt} is the inverse mass of a carbonyl group (0.14585) and the L_{ij} matrix elements, which are taken as a quantitative assessment of the extent of coupling of the two A_1 ν(CO) vibrations, were obtained from the above described vibrational analysis and are noted in Table I. The angle, θ, defines the geometry of the OC_{ax}–M–CO_{eq} arrangement. The μ'_{MCO} values represent a characteristic dipole moment change along the M–CO bond axis (longitudinal) for each symmetry mode.

$$I_{A_1}(1) = (\mu'_{MCO}{}^{(1)}L_{11} + 3^{1/2}(\cos\theta + \rho)\mu'_{MCO}{}^{(2)}L_{21})^2 \quad (2)$$

$$I_{A_1}(2) = (\mu'_{MCO}{}^{(1)}L_{12} + 3^{1/2}(\cos\theta + \rho)\mu'_{MCO}{}^{(2)}L_{22})^2 \quad (3)$$

$$I_E = G_{tt}(\mu'_{MCO}{}^{(3)})^2(3\sin^2\theta) \quad (4)$$

Table I. Calculated and Observed CO Stretching Frequencies in [PPN][HFe(CO)$_4$] in Tetrahydrofuran

Molecule	Symmetry	Obsd[a]	Calcd
All ^{12}CO species	$A_1^{(2)}$	*1997.6*	1996.8
	$A_1^{(1)}$	*1904.7*	1905.0
	E	*1875.8*	1876.0
Mono-^{13}CO, radially substituted	A′	1988.7	1988.2
	A′		1903.1
	A″	1875.8	1876.0
	A′	*1844.7*	1844.0
Mono-^{13}CO, axially substituted	$A_1^{(2)}$	1988.7	1988.5
	$A_1^{(1)}$		1870.3
	E	1875.8	1876.0

[a] The four frequencies (italicized) were used as input and were calculated with an average error of 0.5 cm^{-1} or 0.027%. Force constants calculated were $k_1 = 15.02_2$, $k_2 = 14.71_6$, $k_{c'} = 0.50_6$, and $k_c = 0.36_4$. Calculated values of the L_{ij} matrix elements were $L_{11} = L_{22} = 0.32952$ and $L_{12} = -L_{21} = 0.19303$.

Table II. Infrared Intensities of the Carbonyl Stretching Vibrations in Axially Substituted Iron Tetracarbonyl Derivatives[a]

Compd	Intensity × 10^{-4}, M^{-1} cm^{-2}		
	$A_1^{(2)}$	$A_1^{(1)}$	E
$[HFe(CO)_4]^-$	0.500	11.9	39.4
$(n\text{-}C_4H_9)_3PFe(CO)_4$[b]	4.36	4.59	25.3
$(C_6H_5O)_3PFe(CO)_4$[b]	3.21	5.52	22.4

[a] All measurements were carried out in tetrahydrofuran solution. [b] Taken from ref 11.

If the high-frequency A_1 band involved only the symmetrical stretching of the three equatorial carbonyl groups, there would be no net change in dipole moment and hence no intrinsic infrared intensity. However, as noted in eq 3, there are three ways in which this band can gain intensity: (a) by coupling with the axial carbonyl group motion, (b) through significant departure of the OC_{ax}–M–CO_{eq} bond angle (θ) from 90°, (c) by electronic migration along the threefold axis, i.e., a transverse dipole moment change in the M–L bond designated by the ρ parameter.

This latter contribution (c) arises from a motion of π-electron density in the M–L bond and, therefore, can be neglected in the present case where L equals the hydride ligand (ρ = 0). If we further assume that the dipole moment derivatives for MCO motion involving equatorial carbonyl groups are equal for the two symmetry modes (A_1 and E), i.e., $\mu'_{MCO}{}^{(3)} = \mu'_{MCO}{}^{(2)}$, it is possible to calculate the angle (θ).[14]

At this point it is worth pointing out the qualitative effect on the intensity of the high-frequency band of moving the iron atom out of the plane of the equatorial CO groups. Since this band corresponds to a totally symmetric stretching motion of the four carbonyl ligands (Figure 3), a θ value <90° will result in a enhancement of the band's intensity over that expected from coupling alone. Alternatively, a θ value >90° would lead to a diminution of intensity relative to that anticipated from coupling. The expected ratio of the band intensities of the $A_1^{(2)}$ and $A_1^{(1)}$ vibrations due to coupling alone can be calculated from eq 2 and 3, where θ = 90° and ρ = 0. The computed

Table III. Values of μ'_{MCO}, the MCO Group Dipole Moment Derivatives, and the CO Stretching Force Constants in Axially Substituted Iron Tetracarbonyl Derivatives[a]

Compd	$\mu'_{MCO}{}^{(1)}$	$\mu'_{MCO}{}^{(3)}$	Force constants, mdyn/A			
			k_1	k_2	k_c'	k_c
$[HFe(CO)_4]^-$	8.73	9.49	15.02	14.72	0.50_6	0.36_4
$(n\text{-}C_4H_9)_3PFe(CO)_4$[b]	7.96	7.78	16.11	15.58	0.48_9	0.32_5
$(C_6H_5O)_3PFe(CO)_4$[b]	7.54	7.07	16.48	15.92	0.45_0	0.32_0

[a] The μ'_{MCO}'s are effective group dipole moment derivatives which involve both MC and CO stretching motions. The units employed here are arbitrary; the intensities are expressed in units of 10^4 M^{-1} cm^{-2}, and L and G terms are based on atomic mass units. [b] Taken from ref 11. For the comparable CO force field in the neutral $HCo(CO)_4$ species, see ref 23.

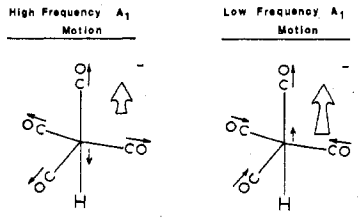

Figure 3. π-electron motion in the M–C–O linkage during the two A_1 motions. The arrows along the M–C–O bond axis represent the changes in internal coordinates during these motions based on the sign convention chosen for the L_{ij} elements. The large arrows indicate the net directions of dipole moment derivatives, both being positive.

ratio, $(L_{12}/L_{11})^2$, is found to be 0.343, a value considerably greater than that observed, 0.0420. It therefore followed from the above discussion that θ is greater than 90°.

We can solve eq 2 and 3 for $\mu'_{MCO}{}^{(1)}$ in terms of the L_{ij} matrix elements and the measured intensities of the two A_1 CO vibrations (eq 5). The relative signs of the quantities $I_1^{1/2}$

$$\mu'_{MCO}{}^{(1)} = \frac{L_{22}I_1^{1/2} - L_{12}I_2^{1/2}}{L_{11}L_{22} - L_{12}L_{21}} \quad (5)$$

and $I_2^{1/2}$ are both taken as being positive (see Figure 3 for the net dipole moment changes). Since the $\sin^2\theta$ changes by only 3% for $\theta = 90 \pm 10°$, it is possible to calculate $\mu'_{MCO}{}^{(3)}$ directly from eq 4.[15] It is then possible to calculate a value for θ employing eq 2 or 3 of 100.2°. This computed angle (θ) is in excellent agreement with Smith and Bau's observed average solid-state value of 99.1°.[5a] In other words, *the solution and solid-state structure of [PPN][HFe(CO)$_4$] are indeed very similar.*

Accurate calculations of angles (to within ±2–3°) in metal carbonyl derivatives based on absolute infrared intensity measurements are generally considered not to be feasible. This is primarily the result of varying contributions to the intensity of the different vibrational modes of π-electronic migration in the metal-substituted ligand bond. However, in cases where there can be no contribution of this type, e.g., in metal hydrides, calculations of angles from intensity data have been very successful.[16-20] For example, the CO_{ax}–Mn–CO_{eq} angle in $HMn(CO)_5$ of 96.5° computed from ν(CO) infrared intensity data by Kaesz and co-workers[21] is in good agreement with that found in the structural determination (97°).[22] Similarly, these researchers reported a calculated angle for the corresponding $HRe(CO)_5$ derivative of 96.7°. We have also computed from intensity measurements obtained by Bor[23] an angle of 101° in $HCo(CO)_4$,[29] the neutral isoelectronic analogue of $[HFe(CO)_4]^-$. The important point in these computations of angles is that a characteristic group dipole moment derivative is obtained for chemically different CO groups.

The calculated group dipole moment derivatives, μ'_{MCO}, for $[HFe(CO)_4]^-$ are listed in Table III along with those of $LFe(CO)_4$ where L = phosphine or phosphite ligands. Included in Table III as well are the CO stretching force constants. Both quantities, F_{CO} and μ'_{MCO}, indicate considerable π-electronic charge placed on the CO groups in the anionic $[HFe(CO)_4]^-$ species as compared with the trivalent phosphorus derivatives, $LFe(CO)_4$. The reversal in order of the magnitudes of $\mu'_{MCO}{}^{(1)}$ and $\mu'_{MCO}{}^{(3)}$ in going from the hydride derivative to the trivalent phosphorus derivatives is due to a charge migration in the M–L (d_π–d_π) bond in these latter cases. In the absence of this effect, electron demand arguments would dictate that $\mu'_{MCO}{}^{(1)}$ be less than $\mu'_{MCO}{}^{(3)}$ as is noted in $[HFe(CO)_4]^-$.

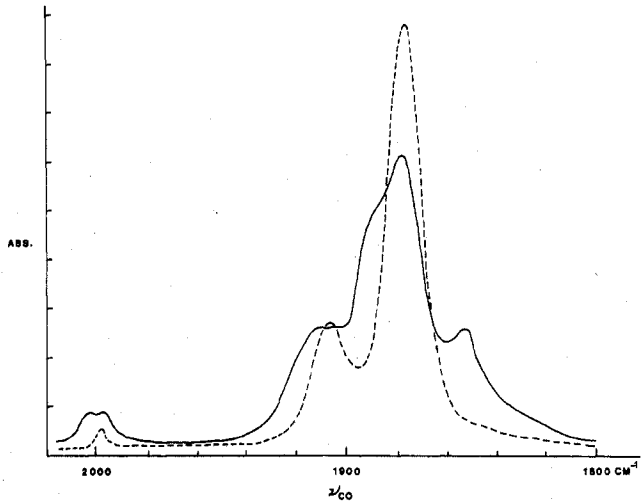

Figure 4. ν(CO) spectra in THF: (–) [PPN][HFe(CO)$_4$], (---) [PPN][HFe(CO)$_4$] (same solution) in the presence of a fourfold excess of $NaBPh_4$.

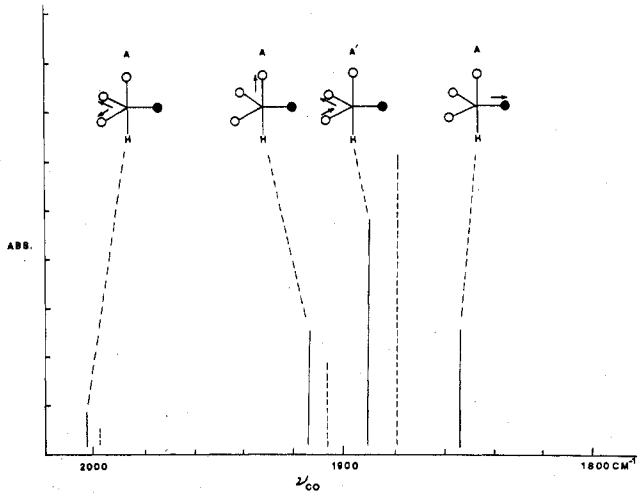

Figure 5. Vibrational assignment of ν(CO) absorptions in the [Na][HFe(CO)$_4$] contact-ion species.

Carbonyl Stretching Force Constants in [Na][HFe(CO)$_4$]. Although the $[HFe(CO)_4]^-$ anion exhibits a symmetrical structure in solution in the presence of the PPN^+ cation, the analogous sodium salt exists as a contact-ion species in THF solution as evidenced by the ν(CO) spectrum (Figure 4). This

Table IV. Calculated Force Constants in Contact Ion Pairs[a]

Compd	Force constant,[b] mdyn/A				
	k_1	k_2	k_3	k_c'	k_c
$Na^+HFe(CO)_4^-$	15.10	14.95	14.23	0.36_4	0.50_6
$Na^+Mn(CO)_4(Me_2PhP)^-$	14.31	13.84	12.94	0.51_3	0.41_1
$Na^+Mn(CO)_4(Ph_3P)^-$	14.39	13.95	13.00	0.47_9	0.40_6
$Na^+Mn(CO)_4((PhO)_3P)^-$	14.56	14.34	13.43	0.54_2	0.35_9

[a] Determined from frequency data in THF. [b] k_3 corresponds to the CO ligand in contact with Na^+. For a description of the force field, see ref 8.

Scheme I

$$Na^+HFe(CO)_4^- + [PPN][BPh_4] \rightleftharpoons PPN^+HFe(CO)_4^- + NaBPh_4$$

$$\downarrow {}^{13}CO \qquad\qquad \downarrow {}^{13}CO$$

$$Na^+HFe(CO)_{4-x}({}^{13}CO)_x \xleftarrow{[PPN][BPh_4]} PPN^+HFe(CO)_{4-x}({}^{13}CO)_x$$

spectrum (Figure 4) was obtained from the metathesis reaction of $NaBPh_4$ and $[PPN][HFe(CO)_4]$ in a ratio of 4 to 1, respectively, and indicates a mixture of $[Na^+\cdots{}^-OCFe(CO)_3H]$ and $[HFe(CO)_4]^-$. A line drawing of the convoluted spectrum is shown in Figure 5 with assignments of bands (2003, 1910, 1890, and 1854 cm^{-1}) due to the sodium hydridoiron tetracarbonyl species being given. Spectral analysis, both with respect to ν(CO) band positions and intensity ratios, indicates interaction of Na^+ with one of the equatorial carbonyl oxygen atoms.

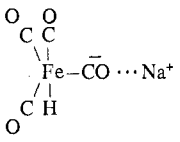

Restricted CO stretching force constant calculations were performed as previously described for the $Na^+Mn(CO)_4L^-$ species.[8] Calculated values for the CO stretching force constants in the $Na^+HFe(CO)_4^-$ contact ion-pair species are listed in Table IV along with comparable $Na^+Mn(CO)_4L^-$ data. The change in ν(CO) force constant upon complexation (k_2 for the solvent-separated or free ion minus k_3) reflects the extent of $MCO\cdots Na^+$ interaction. For the $HFe(CO)_4^-$ derivative this difference ($k_2 - k_3$) is 0.49, whereas in the phosphine and phosphite derivatives of manganese ($k_2 - k_3$) ranges from 0.71 to 0.78, indicating a greater interaction in these latter species. This is consistent with the slightly greater electronegativity of iron over manganese and the donor abilities of phosphines and phosphites as compared to the hydride ligand.

It is interesting to note here that the $Na^+HFe(CO)_4^-$ species was found to readily exchange carbonyl ligands with gaseous ^{13}CO, whereas the $PPN^+HFe(CO)_4^-$ does not. For example, $PPN^+HFe(CO)_4^-$ in the presence of $NaBPh_4$ was observed to be enriched with ^{13}CO upon standing at room temperature (in the dark) in THF saturated with ^{13}CO (Scheme I).[24]

This experiment indicates that the carbonyl ligands in the $HFe(CO)_4^-$ complex are more labile in the presence of specific cation interaction. A similar observation has been reported for $Fe(CO)_5$ in the presence of acid, i.e., $HFe(CO)_5^+$ exchanges CO ligands intermolecularly more readily than $Fe(CO)_5$.[25,26]

Other chemical differences between $HFe(CO)_4^-$ in a symmetrical environment as its PPN^+ salt and in a cation-perturbed environment as its Na^+ salt have been observed. Solutions of $Na^+HFe(CO)_4^-$ in THF are very reactive toward O_2; the half-life for $Na^+HFe(CO)_4^-$ reaction with O_2 at room temperature is on the order of 5 min whereas that for $PPN^+HFe(CO)_4^-$ is on the order of 100 min.[10] Different reaction processes may of course be differently affected by ion-pairing phenomena. For example, essentially the *same* rates of reaction of PPN^+ and Na^+ salts of $HFe(CO)_4^-$ with EtI have been reported, with the PPN^+ salt possibly being the more reactive.[2]

It should be pointed out that conductivity measurements have shown the large PPN^+ cation to be associated with transition metal carbonylates in THF.[10] The ion-pair dissociation constant, as determined from analysis of the dependence of specific conductance on concentration, for the equilibrium described by eq 6, was found to be $K_D = \sim 2 \times 10^{-4}$ M. This is an order of magnitude greater than that expected for $Na^+HFe(CO)_4^-$; the very similar $Na^+Mn(CO)_5^-$ has a K_D of 1.98×10^{-5} M in THF. (The latter salt also displays CO perturbation due to direct $Mn{-}C{\equiv}O\cdots Na^+$ interaction, as determined by infrared.[8]) Nevertheless $PPN^+HFe(CO)_4^-$ ion pairs are expected to be prominent at the concentrations generally used to study reactions.[27,28] It is clear, however, that enough cavity space exists between the PPN^+ and $HFe(CO)_4^-$ to provide an essentially symmetrical electronic environment for $HFe(CO)_4^-$, as indicated by the infrared studies.

$$PPN^+HFe(CO)_4^- \rightleftarrows PPN^+ + HFe(CO)_4^- \qquad (6)$$

In conclusion, it should be emphasized that it is the *specificity* of the ion association in $NaHFe(CO)_4$ which is primarily responsible for the differences in ν(CO) spectral properties and ^{13}CO-exchange reactions observed in the $NaHFe(CO)_4$ and $PPNHFe(CO)_4$ species.

Registry No. $[PPN][HFe(CO)_4]$, 56791-54-9; $[Na][HFe(CO)_4]$, 53558-55-7; $HFe(CO)_3(^{13}CO)^-$(radially substituted), 65024-70-6; $HFe(CO)_3(^{13}CO)^-$(axially substituted), 64957-27-3; $Fe(CO)_5$, 13463-40-6.

References and Notes

(1) R. B. King, *Acc. Chem. Res.*, **3**, 417 (1970).
(2) J. P. Collman, *Acc. Chem. Res.*, **8**, 342 (1975).
(3) J. E. Ellis and R. A. Faltynek, *J. Am. Chem. Soc.*, **99**, 1801 (1977).
(4) R. Pettit, 171st National Meeting of the American Chemical Society, April 1976, New York, N. Y., and 172nd National Meeting of the American Chemical Society, Sept 1976, San Francisco, Calif.
(5) (a) M. B. Smith and R. Bau, *J. Am. Chem. Soc.*, **95**, 2388 (1973); (b) R. D. Wilson and R. Bau, *ibid.*, **96**, 7601 (1974); (c) R. D. Wilson, S. A. Graham, and R. Bau, *J. Organomet. Chem.*, **91**, C49 (1975); (d) H. B. Chin and R. Bau, *J. Am. Chem. Soc.*, **98**, 2435 (1976); (e) R. G. Teller, R. G. Finke, J. P. Collman, H. B. Chin, and R. Bau, *ibid.*, **99**, 1104 (1977).
(6) R. M. Laine, R. G. Rinker, and P. C. Ford, *J. Am. Chem. Soc.*, **99**, 252 (1977).
(7) M. Y. Darensbourg and D. Burns, *Inorg. Chem.*, **13**, 2970 (1974).
(8) M. Y. Darensbourg, D. J. Darensbourg, D. Burns, and D. A. Drew, *J. Am. Chem. Soc.*, **98**, 3127 (1976).
(9) M. Y. Darensbourg and C. Borman, *Inorg. Chem.*, **15**, 3121 (1976).
(10) M. Y. Darensbourg, H. Barros, and C. Borman, *J. Am. Chem. Soc.*, **99**, 1647 (1977).
(11) D. J. Darensbourg, H. H. Nelson, III, and C. L. Hyde, *Inorg. Chem.*, **13**, 2135 (1974).
(12) J. H. Schachtschneider and R. G. Snyder, *Spectrochim. Acta*, **19**, 85, 117 (1963).
(13) D. J. Darensbourg, *Inorg. Chim. Acta*, **4**, 597 (1970).
(14) This in turn assumes that the contributions to the A_1 and E vibrational modes resulting from electron-demand differences are negligible in this case.
(15) It is possible in fact to do an iterative calculation, once an initial value of θ is computed, for μ'_{MCO}(3). This was done to arrive at a self-consistent angle (θ).
(16) This also applies to metal carbonyl fragments where there are no substituted ligands. Examples of angles' calculations from ν(CO) infrared intensity measurements may be found in ref 17–20.
(17) M. A. Graham, M. Poliakoff, and J. J. Turner, *J. Chem. Soc. A*, 2939 (1971).
(18) R. N. Perutz and J. J. Turner, *J. Am. Chem. Soc.*, **97**, 4800 (1975).
(19) H. Huber, E. P. Kündig, G. A. Ozin, and A. J. Poë, *J. Am. Chem. Soc.*, **97**, 308 (1975).
(20) L. A. Hanlan, H. Huber, E. P. Kündig, B. R. McGarvey, and G. A. Ozin, *J. Am. Chem. Soc.*, **97**, 7054 (1975).
(21) P. S. Braterman, R. Bau, and H. D. Kaesz, *Inorg. Chem.*, **6**, 2097 (1967).
(22) S. J. LaPlaca, J. A. Ibers, and W. C. Hamilton, *J. Am. Chem. Soc.*, **86**, 2288 (1964).

(23) G. Bor, *Inorg. Chim. Acta*, **1**, 81 (1967).
(24) Consistent with our results, Collman and co-workers have also reported that $NaHFe(CO)_4$ undergoes exchange with ^{13}CO in solution: J. P. Collman, R. G. Finke, P. L. Matlock, R. Wahren, and J. I. Brauman, *J. Am. Chem. Soc.*, **98**, 4685 (1976).
(25) F. Basolo, A. T. Brault, and A. J. Poë, *J. Chem. Soc.*, 676 (1964).
(26) K. Noack and M. Ruch, *J. Organomet. Chem.*, **17**, 309 (1969).
(27) The concentration of triple ions and higher aggregates is expected to be quite small in THF solutions of $PPN^+HFe(CO)_4^-$. In fact, in the much less bulky and more tightly ion-paired salts, $NaMn(CO)_5$ and $NaMn(CO)_4L$, the ion pair dissociation constants ($\sim 10^{-5}$ M) and the triple ion dissociation constants ($\sim 10^{-3}$ M)[8] may be combined with the mass action expression for pairs and triplets[28] to obtain an estimate of $[CA_2^-]$ and $[C_2A^+]$ of ca. 15% at 0.01 M concentration levels. The $Na^+HFe(CO)_4^-$ is expected to behave similarly to the manganese carbonylates; however, the lack of significant deviation of the $PPN^+HFe(CO)_4^-$ from the Fuoss plot above the triple ion "critical concentration limit"[28] indicates that appreciable aggregation of this salt at the 0.01 M concentration level is unlikely.
(28) R. M. Fuoss and F. Accascina, "Electrolytic Conductance", Interscience, New York, N.Y., 1959.
(29) A recent gas-phase electron diffraction study of $HCo(CO)_4$ has been reported by McNeill and Scholer (*J. Am. Chem. Soc.*, **99**, 6243 (1977)). The average CO_{ax}–Co–CO_{eq} angle found was 99.7°.

Contribution from the Moore School of Electrical Engineering and Laboratory for Research on the Structure of Matter, University of Pennsylvania, Philadelphia, Pennsylvania 19174

Direct Synthesis of Stage 1–3 Intercalation Compounds of Arsenic Pentafluoride in Graphite

E. R. FALARDEAU,* L. R. HANLON, and T. E. THOMPSON

Received December 29, 1976

Uniform stage 1–3 AsF_5–graphite intercalation compounds were prepared by direct interaction of AsF_5 vapor with highly oriented pyrolytic graphite under isothermal conditions. The compounds were characterized using x-ray and gravimetric analyses coupled with observation of the *c*-axis thickness increase. The *c*-axis repeat distance, I_c, followed the relation $I_c = (4.75 + n3.35)$ Å, where n = stage. The stoichiometry of stages 1–3 corresponded to $C_{8n}AsF_5$. The *c*-axis thickness increase proved to be a reliable indicator of stage for stages 1–3; however, more dilute materials were invariably inhomogeneous.

Intercalation is the process of inserting foreign atoms or molecules between the layers of a lamellar host material. Although intercalation of graphite has been known for over 40 years and many types of atoms and molecules have been intercalated,[1,2] no definitive explanation exists for the chemical bonding involved.

Currently, there are two major interests in graphite intercalation compounds. First, in the intercalation process the reactivity of the intercalant is severely modified,[3] hence potential use in selective catalysis can be envisioned. Second, intercalation compounds are synthetic metals.[1,2] They display properties typical of metals, especially high infrared reflectance and high electrical conductivity.

As part of a broad-based investigation into the solid-state properties of graphite intercalation compounds, we have synthesized the first uniform-stage compounds of highly oriented pyrolytic graphite (HOPG) and AsF_5. The stoichiometry of these compounds was observed to be $C_{8n}AsF_5$, where n = stage. (Stage is the number of contiguous carbon layers between successive intercalant layers). Earlier investigators utilizing grafoil and powdered graphite reported the formation of an ASF_5 graphite compound of stoichiometry $C_{10}AsF_5$.[4] However, while their published x-ray data indicated that intercalation had occurred, it did not indicate the formation of a unique stage material.

Recent measurements on uniform AsF_5–graphite compounds have shown that the basal-plane (*a* axis) electrical conductivity can be as high as that of silver,[5] the best elemental conductor. Since the envionmental stability of the higher stage compounds is promising,[6] AsF_5–graphite is a potentially practical synthetic metal. The synthesis of these compounds is the subject of this paper.

Experimental Section

The material used throughout this work was highly oriented pyrolytic graphite (HOPG) which was obtained from Union Carbide and used without further purification. The spread of the *c* axes in this polycrystalline material is of the order of 1° and the crystallite sizes are of the order of a few microns. Most of the graphite samples to be intercalated were cut to 5 × 8 mm² *c*-face rectangles using a 0.025-cm diamond string saw. Additional samples from 5 × 5 mm² to 6 × 20 mm² were also intercalated; many of these were cut to size using air abrasion instead of the string saw. The initial thickness of most samples was in the range 0.025–0.064 cm; these *c*-axis thickness measurements were made using a microscope with a calibrated reticule (sensitivity = 5 × 10^{-4} cm). The initial weight of the samples fell in the range 15–50 mg (±0.05 mg).

The arsenic pentafluoride (Ozark Mahoning) was checked for purity by vapor-phase molecular weight determinations. In most instances it was found acceptable as received (±1% of theoretical value 169.9); when unacceptable it was purified by trap-to-trap distillation and rechecked.

All volatile materials were manipulated utilizing standard high-vacuum techniques in a glass system equipped with glass–Teflon valves. All intercalated materials were handled under a dry nitrogen atmosphere since the lowest stage compounds exhibited extreme sensitivity to moisture.

All AsF_5–graphite intercalation compounds were prepared in an inverted h-shaped Pyrex reactor equipped with a glass–Teflon valve on the side arm. The main reactor tube was made of 0.5-in. o.d. glass, the top of which was fitted with a Swagelok ss plug fitted with Teflon ferrules. This arrangement allowed easy insertion of the solid graphite reactant and removal of the intercalated product from an otherwise closed system. The typical total volume of these reaction vessels was 10 mL. Reactions containing up to 3.6 atm of AsF_5 were successfully executed without leakage through the Swagelok connection. The sample of graphite to be intercalated was supported in the reactor in a loose Pt wire spiral which performed two functions. First, it held the graphite in a stable position such that consistent thickness measurements could be made in situ. Second, it suspended the graphite above the bottom of the reactor. This second function enabled the intercalation process to proceed entirely in the vapor phase without contact with AsF_5 liquid during the initial warming process.

In a typical reaction a known amount of AsF_5 (0.5–1.5 ± 0.03 mmol) was condensed at −196 °C into the bottom of the reaction vessel containing the suspended graphite. Since only the bottom of the vessel was cooled the graphite did not vary appreciably from room temperature. The reaction was started by allowing the AsF_5 to warm to 23 °C, at which temperature it is all in the vapor state. The initial warming period mentioned above, during which the AsF_5 warms from −196 to +23 °C, was typically less than 2 min. No observable reaction (thickness) occurred during this time. For a typical 35-mg sample and initial pressure of 1 atm, the final pressure was 0.5 atm over a

0020-1669/78/1317-0301$01.00/0